Journal of Natural Sciences and Mathematics Research
J. Nat. Scien. & Math. Res. Vol. 12 No. 1 (2026) 87-99
ISSN: 2460-4453 (Online); 2614-6487 (Printed)
Available online at http://journal.walisongo.ac.id/index.php/jnsmr

In silico physicochemical and drug-likeness assessment of Indoloquinoxaline Derivatives as potential Anti-Alzheimer Agents

Annisha Noor Dienna[1*], Alfa Zihni Adzaky[1], David Ardiansyah[1], Annisa Ananda[1], and Muhammad Zulqurnain[2]

[1] Department of Chemistry, Faculty of Mathematics and Natural Sciences, Universitas Lampung, Indonesia
[2] Department of Chemistry Education, Faculty of Teacher Training and Education, Universitas Sriwijaya, Indonesia

* Corresponding author's e-mail: annishandienna@fmipa.unila.ac.id

ABSTRACT

Alzheimer's disease (AD) remains a major progressive neurodegenerative disorder with limited therapeutic efficacy, primarily targeting acetylcholinesterase (AChE), with significant challenges related to Blood-Brain Barrier (BBB) penetration. This study aimed to perform drug likeness screening, ADMET profiling, and BBB penetration prediction of indoloquinoxaline derivatives as potential CNS-active anti-Alzheimer candidates using SwissADME as the sole computational platform. A total of 36 compounds, comprising 31 indoloquinoxaline derivatives and five reference anti-Alzheimer drugs, were analyzed in silico using five pharmacokinetic filters (Lipinski, Ghose, Veber, Egan, and Muegge), followed by lipophilicity assessment (Consensus LogP range: 2.59–5.39), molecular weight, rotatable bonds, hydrogen bonding, and medicinal chemistry evaluations. All 36 compounds fulfilled Lipinski and Veber criteria with 100% compliance, while Ghose, Egan, and Muegge filters identified 3, 2, and 8 violations, respectively, predominantly attributable to excessive lipophilicity in substituents such as $-CF_3$ and tert-butyl groups. The investigated compounds exhibited CNS-compatible MW (219.24–400.52 Da), LogP (2.88–4.95 for the majority), and TPSA (30.71–54.50 $Å^2$) profiles. A total of 29 out of 31 synthesized compounds (93.5%) were predicted as BBB-permeant. In addition, all candidates showed zero PAINS alerts and predominantly zero Brenk alerts, indicating favorable medicinal chemistry characteristics and low risk of nonspecific bioassay interference. Several compounds demonstrated physicochemical properties comparable to clinically approved anti-Alzheimer drugs (donepezil, galantamine, rivastigmine), suggesting promising potential for further AChE-targeted CNS drug development.

Keywords:
Alzheimer's disease; drug likeness; indoloquinoxaline derivatives; medicinal chemistry; SwissADME.
Subject Classification Code: (Computational Chemistry)

Introduction

The importance of therapeutic approaches are required to treat the multiple pathological mechanisms of Alzheimer's disease, a progressive neurodegenerative disorder characterized by cholinergic deficit, amyloid-β accumulation, and tau hyperphosphorylation (Reddi Sree et al., 2025). The indoloquinoxaline derivative compounds have a growing interest in CNS drug discovery due to their fused aromatic ring system, which facilitates acetylcholinesterase inhibition, blood-brain barrier penetration, and potential multitarget interactions (Hamulakova et al., 2021). Computational tools such as SwissADME have therefore become essential in early-stage anti-Alzheimer screening by enabling rapid, accessible assessment of drug-likeness, ADMET profiles, and CNS suitability without requiring extensive laboratory resources.

Studies employing SwissADME-based evaluation have demonstrated its practical utility for drug-likeness and ADMET screening (Antoine), but most remain limited to single-filter assessments such as Lipinski's Rule of Five without BOILED-Egg predictions, or medicinal chemistry alerts as part of a unified screening approach. Studies employing SwissADME-based evaluation have demonstrated its practical utility for drug-likeness and ADMET screening, but most remain limited to single-filter assessments such as Lipinski's Rule of Five without BOILED-Egg predictions, or medicinal chemistry alerts as part of a common screening approach. Despite indoloquinoxaline derivatives' structural features relevant to BBB penetration and cholinergic target interaction but underexplored in SwissADME-based CNS screening. The evaluation of lipophilicity, BBB permeability indicators, drug-likeness filters, and ADMET parameters for indoloquinoxaline compounds in a structured and comparable manner is the gap highlighted for a dedicated SwissADME-based profiling study.

The present study was therefore designed to perform SwissADME-based physicochemical and pharmacokinetic profiling of indoloquinoxaline derivatives as potential anti-Alzheimer candidates. Specifically, this study evaluated drug-likeness through Lipinski, Veber, Ghose, and Egan filters; estimated BBB permeability. This approach is aligned with accessible computational strategies suitable for early-stage CNS drug discovery, particularly in resource-limited research settings, and provides a structured SwissADME-based assessment of indoloquinoxaline derivatives, a topic that remains relatively underexplored in the current literature. Indoloquinoxaline derivatives represent a structurally privileged scaffold in this context, combining the planar fused ring geometry necessary for intercalative or active-site AChE binding with inherent physicochemical tunability at multiple substitution positions. Computational tools, particularly SwissADME, provide an accessible and validated platform for high-throughput simultaneous assessment of these parameters via integrated drug-likeness filters, lipophilicity models, and a BBB prediction model (Bitew et al., 2021; Khwaza et al., 2025). The application of such a platform to the indoloquinoxaline series therefore represents both a practical pharmacokinetic screening strategy and a necessary scientific step toward translating structural novelty into developable drug candidates with defined CNS bioavailability potential.

Methods

This study was conducted entirely in silico using the SwissADME web platform (swissadme.ch, accessed March 2026). A total of 36 compounds were evaluated: 31 indoloquinoxaline derivatives from Kanhed et al. (2022) and five reference drugs (donepezil, galantamine, memantine, rivastigmine, tacrine). Derivatives were selected based on three criteria: complete bioactivity data, unambiguous SMILES notation, and structural diversity across the indoloquinoxaline scaffold. Reference drugs served as pharmacokinetic benchmarks. The novelty of this study lies in providing the first systematic SwissADME-based profiling of indoloquinoxaline derivatives as a compound class, which has not been previously reported. All 36 SMILES were submitted individually to the SwissADME server for descriptor calculation.

Physicochemical and pharmacokinetic properties were predicted via SwissADME (Daina et al., 2017). Evaluated descriptors included MW (≤500 Da), TPSA (≤140 $Å^2$), NRB (≤10), HBA (≤10), and HBD (≤5), consistent with CNS drug-likeness criteria (Staneva et al., 2024). Lipophilicity was assessed using five SwissADME consensus models, with a CNS-optimal range of $1 \leq \text{LogP} \leq 3$ Hassan Pajouhesh. Water solubility was classified using the ESOL; BBB permeability and GI absorption were predicted via SwissADME.

Drug-likeness was assessed using five SwissADME filters. The Lipinski Rule of Five (MW ≤500, LogP ≤5, HBD ≤5, HBA ≤10) served as the primary filter; violations of more than one criterion were classified as unfavorable (Miebs et al., 2024). Supplementary filters included Veber (NRB ≤10, TPSA ≤140 $Å^2$) (Veber et al., 2002), Ghose (160–480 Da, LogP −0.4 to 5.6), Egan (TPSA ≤131.6 $Å^2$, LogP ≤5.88), and Muegge (MW 200–600, LogP −2 to 5) (Kralj et al., 2023). Results were compared descriptively with reference drugs. All SwissADME outputs were recorded in Microsoft Excel for tabulation. The overall workflow followed four sequential steps as presented in Figure1.

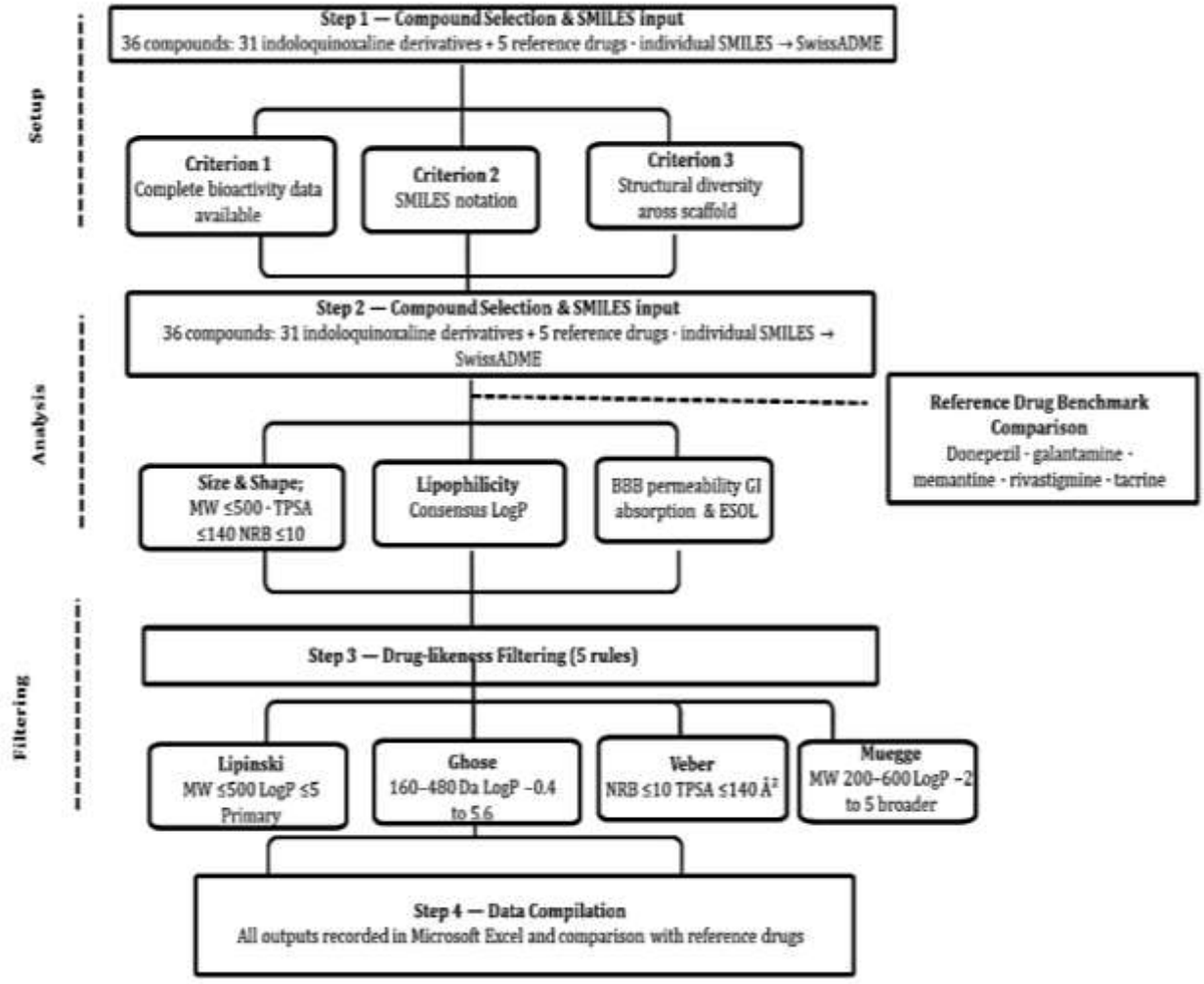

Figure 1. Workflow of SwissADME-Based Drug-Likeness, ADMET, and BBB Permeability Evaluation of Indoloquinoxaline Derivatives and Reference Anti-Alzheimer Drugs

Results and Discussions

Drug-Likeness Evaluation of Candidate Compounds

The drug likeness of all candidate compounds was evaluated based on five widely recognized pharmacokinetic filter criteria: Lipinski's Rule of Five, Ghose filter, Veber filter, Egan filter, and Muegge filter, as summarized in Table 1 and Table 2. These filters assess oral bioavailability and absorption potential based on physicochemical descriptors including MW, LogP, HBA, HBD, TPSA, RB, and MR.

The Lipinski Rule of Five requires MW ≤ 500 Da, LogP ≤ 5, HBA ≤ 10, and HBD ≤ 5 (Sampat et al., 2022). All 36 candidate compounds (100% compliance) satisfied these criteria without a single violation, indicating favorable passive intestinal permeability and oral bioavailability potential across the entire series. Similarly, the Veber filter (RB ≤ 10, TPSA ≤ 140 $Å^2$) (Vawhal & Jadhav, 2022), was satisfied by all 36 compounds (100% compliance), confirming that molecular flexibility and polarity are within acceptable ranges for good oral absorption.

The Ghose filter, applying more stringent boundaries (MW 160–480 Da, WLOGP −0.4 to 5.6, MR 40–130, atom count 20–70) (Mahmud et al., 2022), revealed three violations: compounds 3i, 3l, and 7j (91.67% compliance). Compound 3i (WLOGP > 5.6, MR = 103.29) partially exceeds acceptable limits due to a trifluoromethyl ($–CF_3$) substituent that increases lipophilicity and molecular refractivity. Compound 3l WLOGP > 5.6, MR = 117.58) bears a bulky tert-butyl group that substantially elevates hydrophobic surface area and MR. Compound 7j (WLOGP > 5.6, MR =

108.11) contains a para-chlorobenzyl substituent with a benzimidazole core whose combined aromatic and halogenated framework elevates MR beyond the permitted range.

Table 1. Drug-Likeness Evaluation of Candidate Compounds Based on Lipinski, Ghose, Veber, Egan, and Muegge Filters

Drug-Likeness Parameter	Number of Compounds Meeting Criteria	Number of Violations	Compliance Percentage	Compounds Not Meeting Criteria
Lipinski	36	0	100%	–
Ghose	33	3	91.67%	3i, 3l, 7j
Veber	36	0	100%	–
Egan	34	2	94.44%	3i, 3l
Muegge	28	8	77.78%	3g, 3i, 3k, 3l, 7j, Memantine, Tacrine

Table2. Physicochemical Parameters of Compounds Violating Drug-Likeness Filters and Reference Drugs

Compound	Violated Filter(s)	MW (Da)	Consensus LogP	HBA	HBD	TPSA (Å²)	RB	MR
3g	Muegge	388.26	4.77	2	0	30.71	2	105.99
3i	Ghose, Egan, Muegge	377.36	5.22	5	0	30.71	3	103.29
3k	Muegge	323.39	4.52	2	0	30.71	2	103.26
3l	Ghose, Egan, Muegge	365.47	5.39	2	0	30.71	3	117.58
7j	Ghose, Muegge	357.84	4.88	2	0	30.71	3	108.11
Memantine	Muegge	179.30	2.85	1	1	26.02	0	55.68
Tacrine	Muegge	198.26	2.59	1	1	38.91	0	63.58
Donepezil	Pass All Filters	379.49	4.00	4	0	38.77	6	115.31
Galantamine	Pass All Filters	287.35	1.92	4	1	41.93	1	84.05
Rivastigmine	Pass All Filters	250.34	2.34	3	0	40.49	4	73.12

The Egan filter (WLOGP ≤ 5.88, TPSA ≤ 131.6 Å²) (Rashid et al., 2023) identified two violations involving compounds 3i and 3l (94.44% compliance). 3i and 3l have WLOGP values of >5.88, driven by $-CF_3$ and tert-butyl substituents, respectively, pushing them beyond the acceptable lipophilicity window, suggesting potential reduction in membrane permeability and oral absorption efficiency despite satisfactory hydrogen bonding characteristics.

The Muegge filter, incorporating the broadest structural constraints (MW 200–600 Da, XLOGP3 of −2 to 5, TPSA ≤ 150 Å², rings ≤ 7, RB ≤ 15, HBD ≤ 5, HBA ≤ 10) (Lambev et al., 2025), yielded the highest number of violations with eight non-compliant compounds (77.78% compliance), including 3g, 3i, 3k, 3l, 7j, Memantine, and Tacrine. Failures among candidate compounds are primarily attributed to LogP exceeding the 5.0 threshold: 3g,3k, 3i, 3l, and 7j have XLOGP3 > 5. Notably, Memantine (MW = 179.30) and Tacrine (MW = 198.26) failed due to MW falling below the 200 Da minimum, illustrating that even approved drugs may not satisfy all filter criteria simultaneously, a recognized limitation of rule-based assessments. The structure of the compounds as shown in the Figure 2.

The three approved cholinesterase inhibitor reference drugs such as, Donepezil, Galantamine, and Rivastigmine, passed all five filters, with MW values of 379.49, 287.35, and 250.34 Da, moderate LogP values (4.00, 1.92, and 2.34), and TPSA below 45 Å², validating these filters as robust benchmark tools.

3g

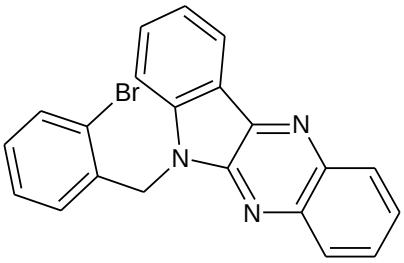

3i

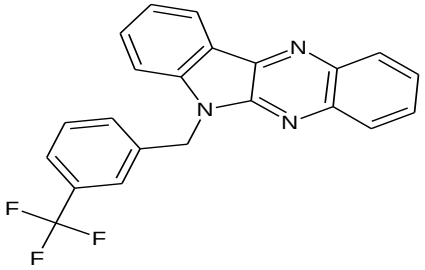

3k

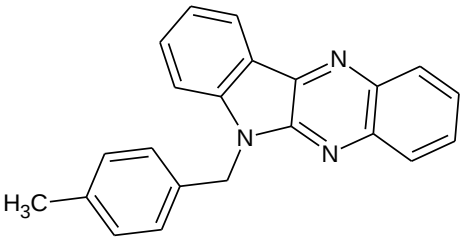

3l

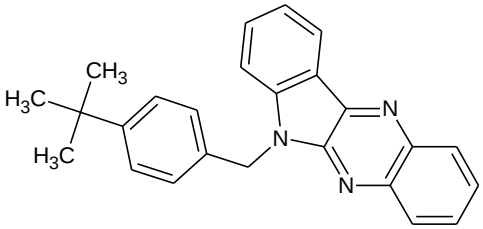

7j

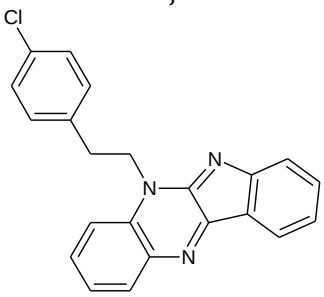

Memantine

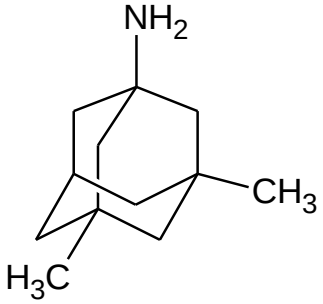

Tacrine

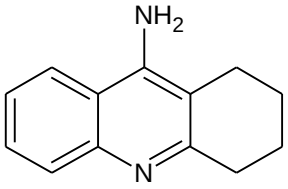

Donepezil

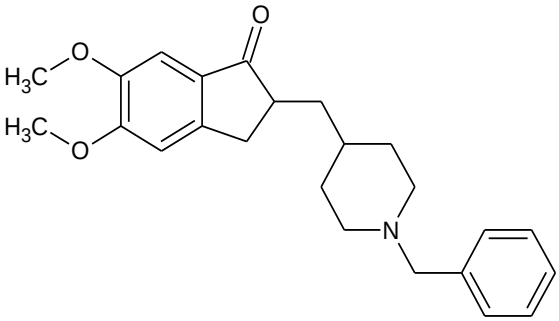

Galantamine

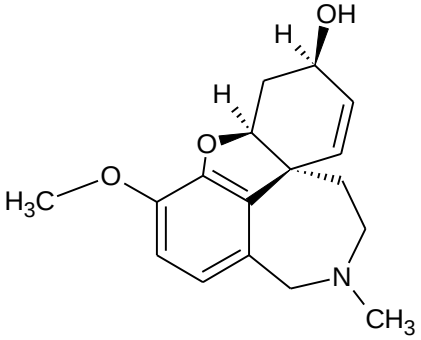

Rivastigmine

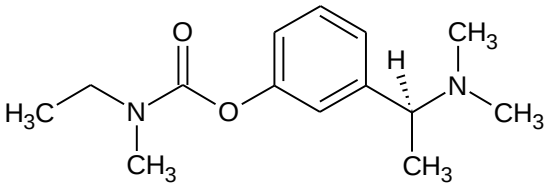

Figure 2. The structure of the compounds

Comparative Analysis of Approved Anti-Alzheimer Drugs and Candidate Compounds

Donepezil-Like Compounds

Among all synthesized candidates, the donepezil-like series demonstrates the closest structural and physicochemical correspondence to donepezil, the most widely prescribed AChEI for mild-to-moderate Alzheimer's disease. Donepezil has LogP 4.00, MW 379.49 Da, TPSA 38.77 Å², MR 115.31, HBA 4, HBD 0, NRB 6, and Log S −4.53. The donepezil-like series mirrors this profile with LogP 3.98–4.95, MW 309.36–400.52 Da, TPSA of 30.71–54.50 Å², HBA 2–4, HBD 0, NRB 2–7, and Log S −5.91 to −4.08. The slight upward LogP shift in certain analogues may enhance membrane partitioning and CNS residence time. The HBD count of zero across the entire series replicates a key pharmacokinetic advantage of the parent drug, eliminating desolvation penalties at the BBB (Xiong et al., 2021). The TPSA range consistently falls below the 90 Å² CNS permeability threshold (Cornelissen et al., 2023), while the MR range of 98.25–126.77 brackets the reference value of 115.31, confirming that compound polarizability remains within pharmacologically productive space. A physicochemical fingerprint precisely tuned to replicate the CNS-optimized profile of a frontline clinical agent was presented by this series, supporting further development.

Rivastigmine-Like Compounds

The rivastigmine-like analogues (3b–3e) are characterized by lower MW, improved aqueous solubility, and compact TPSA, aligning closely with rivastigmine (MW = 250.34 Da, LogP = 2.34, TPSA = 32.78 Å², Log S = −2.33). These analogues extend the reference profile with LogP of 2.94–3.93, MW 233.27–275.35 Da, TPSA 30.71 Å², HBD 0, NRB 0–3, and Log S −3.91 to −3.22. The slightly elevated LogP positions these compounds more centrally within the optimal CNS corridor of 2–5, potentially improving membrane permeability without sacrificing solubility (Pajouhesh & Lenz, 2005). The reduced NRB range of 0–3 versus rivastigmine's 6 indicates greater conformational rigidity, associated with improved CNS selectivity, reduced entropic binding penalties, and greater metabolic stability (Basagni et al., 2023). The TPSA of 30.71 Å² strongly supports passive transcellular BBB permeation, consistent with the predicted BBB permeability of Yes for all analogues. The comparatively higher Log S values suggest superior aqueous solubility relative to the donepezil like series, expected to yield more predictable oral absorption and lower gastrointestinal precipitation risk. Combined with predicted high GI absorption, the rivastigmine-like analogues present an optimized profile for rapid systemic exposure and CNS bioavailability, making them attractive candidates for further ADMET and cholinesterase inhibition studies.

Tacrine Like Compound

Table 4 show comparative SwissADME profiles of candidate compounds and reference drugs. Compound 3a is structurally related to tacrine, the first approved AChEI, later withdrawn due to hepatotoxicity, whose pharmacophoric core retains exceptional AChE inhibitory potency. Tacrine exhibits LogP 2.59, MW 198.26 Da, TPSA 38.91 Å², HBD 1, NRB 0, and Log S −2.98. Compound 3a presents LogP 2.88, MW 219.24 Da, TPSA 41.57 Å², HBD 1, NRB 0, and Log S −3.89. The marginal LogP increase remains well within the CNS window, and the slightly elevated TPSA is inconsequential as both values fall far below the 90 Å² BBB permeability ceiling (Dehnbostel et al., 2024). Zero rotatable bonds in 3a replicate tacrine's conformational rigidity, favoring entropic binding efficiency and metabolic stability (Evangelista et al., 2021). The retained HBD count of one represents a pharmacokinetic concern (Kenny, 2022), yet predicted BBB permeability remains Yes with high GI absorption, suggesting that the NH moiety does not prohibit CNS penetration, likely due to intramolecular conformational masking (Xiong et al., 2021). The slight Log S decrease to −3.89 remains compatible with adequate oral bioavailability. Importantly, the modest MW increase and adjusted polarity in compound 3a represent the type of scaffold optimization historically employed to decouple tacrine's potent AChE inhibitory activity from its hepatotoxic liability, lending biological rationale to its evaluation as a potentially safer tacrine inspired candidate.

Table 4. Comparative SwissADME Profiles of Candidate Compounds and Reference Drugs

Parameter	Donepezil	Donepezil like (3f, 3g, 3h, 3j, 3k, 7a, 7b, 7c, 7d, 7e, 7f, 7g, 7h, 7i, 7j, 7k, 9a, 9b, 9c, 9d, 9e, 9f, 10a, 10b)	Galantamine	Memantine	Rivastigmine	Rivastigmine like (3b, 3c, 3d, 3e)	Tacrine	Tacrine like (3a)
Consensus LogP	4.00	3.98–4.95	1.92	2.85	2.34	2.94–3.93	2.59	2.88
Molecular Weight	379.49	309.36–400.52	287.35	179.30	250.34	233.27–275.35	198.26	219.24
TPSA (Å²)	38.77	30.71–54.50	41.93	26.02	32.78	30.71	38.91	41.57
Molar Refractivity	115.31	98.25–126.77	84.05	55.68	73.12	73.80–88.22	63.58	68.90
GI	High	High	High	High	High	High	High	High
BBB	Yes	Yes	Yes	Yes	Yes	Yes	Yes	Yes
Rotatable Bonds	6	2–7	1	0	6	0–3	0	0
H-Bond Acceptors	4	2–4	4	1	3	2	1	2
H-Bond Donors	0	0	1	1	0	0	1	1
Log S (ESOL)	−4.53	−5.91 – −4.08	−2.72	−2.83	−2.33	−3.91 – −3.22	−2.98	−3.89

The Relationship of LogP, BBB and Molecular Weight

In CNS drug development, the primary pharmacokinetic bottleneck was described as the blood brain barrier. Unlike peripheral tissues where drugs access targets via leaky capillaries, CNS drug delivery is governed by the restrictive paracellular architecture of brain endothelial cells, which necessitates transcellular lipophilic diffusion for passive BBB penetration(Gupta et al., 2024).

The SwissADME BBB permeability prediction model, based on a multi-parameter optimization approach integrating LogP, MW, TPSA, and charge state, categorized 29 out of 31 compounds (93.5%) as BBB permeant. From Table 2, only compounds 3i (LogP = 5.22; TPSA = 30.71 Å²) and 3l (LogP = 5.39; TPSA = 30.71 Å²) were classified as non-BBB permeant, primarily attributable to excessive lipophilicity beyond the productive CNS range, which paradoxically impairs aqueous diffusion and predicts sequestration in vascular lipid components rather than transcellular passage. Structurally, this outcome is directly traceable to the nature of the N-benzyl substituents appended at the indole nitrogen of the β-carboline–quinoxaline scaffold. Compound 3i bears a 3-(trifluoromethyl)benzyl group, in which the strongly electron-withdrawing $–CF_3$ moiety at the meta position dramatically enhances the overall hydrophobic character of the molecule by increasing the lipophilic surface area contributed by the fluorinated aryl ring, despite the fluorine atoms themselves being electronegative. Compound 3l, conversely, incorporates a 4-tert-butylbenzyl group, whereby the bulky, branched alkyl chain introduces pronounced steric hydrophobicity at the para-position of the pendant phenyl ring. In both cases, the appended substituents amplify the intrinsic lipophilicity of the tricyclic β-carboline–quinoxaline core beyond the productive CNS threshold, tipping the LogP above 5.0 and rendering the compounds pharmacokinetically disadvantaged for brain penetration despite their otherwise favorable TPSA. These structural observations carry a direct medicinal chemistry implication: replacement of the $–CF_3$ or tert-butyl moieties in 3i and 3l with moderately lipophilic or hydrogen bond-accepting substituents, such as $–OCH_3$, –F, $–CH_3$, would be expected to recalibrate LogP into the

2–5 range while preserving the aromatic pharmacophore geometry required for AChE active site complementarity.

A non-linear parabolic profile represents a relationship between LogP and BBB permeation. LogP values under 1 describe the compound's hydrophilicity that prevents insertion into the apical membrane lipid bilayer, effectively barring passive diffusion. Conversely, at values more than 5 , excessive lipophilicity increases cellular membrane partitioning but reduces the driving force for diffusion across the aqueous cytoplasm and subsequent exit at the basolateral membrane, a phenomenon well-characterized in the context of P-glycoprotein efflux susceptibility [Małgorzata Janicka]. The productive BBB LogP window of 1–5, with a core optimum of 2–4, is precisely where 87.1% of the present compound library resides, a finding that substantively de-risks the series from a CNS penetration perspective. The remaining 12.9%, represented exclusively by 3i and 3l and above this boundary (LogP 5.22 and 5.39, respectively), a deviation that, while rendering them computationally non-BBB permeant under current prediction criteria, does not preclude their utility as lead structures for lipophilicity-attenuating structural optimization in subsequent medicinal chemistry cycles.

Molecular weight exerts a synergistic constraint on BBB penetration. The widely adopted MW threshold for CNS drugs is ≤450 g/mol (Janicka et al., 2024), more restrictive than Lipinski's general ≤500 g/mol criterion. All 31 compounds satisfy this stringent CNS-specific cutoff, with MWs spanning 219.24–400.52 g/mol, and 29 compounds remaining below 400 g/mol. The heaviest compound in the series, 10b (MW = 400.52 g/mol), still respects the CNS MW limit while maintaining optimal lipophilicity (LogP = 4.44), thereby representing a fully drug like CNS candidate by combined MW and LogP criteria. In the specific context of 3i and 3l, it is notable that their exclusion from the BBB-permeant category is driven purely by excessive LogP rather than by MW violation, their molecular weights of 379 Da and 371 Da, respectively, remain well within acceptable CNS limits, underscoring that lipophilicity control, rather than size reduction, constitutes the primary structural intervention required to rehabilitate these two compounds within the BBB-permeant chemical space.

TPSA, GI Absorption, and the CNS Permeability

Topological polar surface area (TPSA), defined as the sum of surface contributions of polar atoms (primarily oxygen, nitrogen, and their associated hydrogens), is a critical determinant of both intestinal membrane permeation and BBB transcellular transport. The empirically established TPSA thresholds diverge substantially between peripheral GI absorption (TPSA < 140 $Å^2$ for high absorption) and CNS penetration (TPSA < 90 $Å^2$, with an optimal range of 40–90 $Å^2$ for maximal BBB passage) (Dehnbostel et al., 2024).

Table 5 show all 31 synthesized compounds exhibit TPSA values well within both thresholds, ranging from 30.71 $Å^2$ to 54.50 $Å^2$. This uniformly low TPSA profile is mechanistically significant: at TPSA < 60 $Å^2$, passive transcellular diffusion through the BBB is maximally facilitated, with minimal contribution from active efflux transport required for BBB penetration. In contrast, compounds with TPSA approaching 90 $Å^2$ begin to exhibit markedly attenuated CNS exposure in in vivo models, and those exceeding 120 $Å^2$ are effectively excluded from the CNS (Shityakov et al., 2013). The TPSA values of the five reference drugs corroborate this framework: donepezil (38.77 $Å^2$), galantamine (41.93 $Å^2$), memantine (26.02 $Å^2$), rivastigmine (32.78 $Å^2$), and tacrine (38.91 $Å^2$) all display TPSA values in the 26–42 $Å^2$ range, and all are experimentally confirmed BBB-permeable agents.

Regarding GI absorption, 29 of the 31 synthesized compounds are predicted to exhibit high oral gastrointestinal absorption. The two exceptions are compound 3i (LogP = 5.22; Log S = −6.07; GI = Low) and compound 3l (LogP = 5.39; Log S = −6.49; GI = High), which present an apparent inconsistency warranting brief discussion. Both compounds share an identical TPSA of 30.71 $Å^2$, and classical ADMET theory would predict comparable intestinal permeability under equal polarity conditions. Furthermore, compound 3i possesses marginally better aqueous solubility (Log S = −6.07) and slightly lower lipophilicity (LogP = 5.22) than 3l (Log S = −6.49; LogP = 5.39), which, under conventional reasoning, positions 3i as the pharmacokinetically superior compound, or at minimum, equivalent to 3l in GI absorption. The observed reversal,

wherein 3i is classified as a low GI absorber while 3l retains a high GI classification, cannot be fully reconciled through TPSA or Log S parameters alone. This discordance most likely reflects the internal weighting algorithm of the SwissADME GI absorption classifier, which may integrate additional molecular descriptors beyond TPSA and Log S.

Table 5. The Properties of Compound 3i and 3l

Compound	Consensus LogP	Molecular Weight	TPSA (Å²)	Molar Refractivity	GI	BBB	Rotatable Bonds	H Bond Acceptors	H Bond Donors	Log S (ESOL)
3i	5.22	377.36	30.71	103.29	Low	No	3	5	0	−6.07
3l	5.39	365.47	30.71	117.58	High	No	3	2	0	−6.49

P-glycoprotein Substrate Profile and Metabolic Stability

P-glycoprotein (P-gp) Substrate Profile

P-glycoprotein (P-gp), encoded by ABCB1 and expressed on brain endothelial cells, functions as an ATP-dependent efflux transporter that expels xenobiotics from the CNS (Hathcock et al., 2024). Compounds classified as P-gp substrates are subject to active counter-transport at the BBB, potentially reducing net CNS exposure despite favorable passive permeability (Ronaldson & Davis, 2024). In this study, 34 of 36 entries are predicted as P-gp substrates, indicating a theoretical efflux liability across the majority of the series. Only memantine and rivastigmine are classified as non-substrates, consistent with their clinical CNS bioavailability and comparatively lower LogP values (2.85 and 2.34, respectively) and MW below the molecular complexity threshold typically associated with P-gp affinity. For the synthesized P-gp substrates, this prediction does not disqualify them as CNS candidates like donepezil, galantamine, and tacrine are themselves P-gp substrates yet remain clinically effective, but it underscores that in vivo brain concentrations may be influenced by efflux activity, warranting P-gp attenuation strategies in subsequent lead optimization.

CYP450 Inhibition Profile and Implications for Metabolic Stability

Table 6 shoe the properties of compound 3i and 3l. CYP450 enzymes constitute the primary hepatic machinery for biotransformation of CNS-active drugs (Hossam Abdelmonem et al., 2024). Predicting CYP inhibition is critical for two reasons: CYP inhibition may impair metabolism of drugs, generating pharmacokinetic drug–drug interactions (DDIs); and compounds that are CYP substrates may undergo rapid first-pass metabolism, reducing systemic and CNS exposure. SwissADME predictions across five major isoforms are summarized in Table 6.

CYP1A2 from 36 entries; 32 are predicted CYP1A2 inhibitors; only donepezil, galantamine, memantine, and rivastigmine are non-inhibitors. CYP1A2 metabolizes CNS-relevant substrates including clozapine and olanzapine, and its inhibition carries meaningful DDI risk in patients receiving concomitant psychiatric medications (Merino et al., 2022). The non-inhibitor status of four reference drugs suggests CYP1A2 inhibitory activity in the synthesized series is a scaffold-emergent property rather than an intrinsic feature of anti-Alzheimer pharmacophores, warranting DDI consideration given common polypharmacy in Alzheimer's patients.

CYP2C19, from Twenty-seven compounds are predicted CYP2C19 inhibitors, 9 are non-inhibitors, including all five reference drugs and synthesized compounds 3a, 9c, 9e, and 9f. CYP2C19 governs the metabolism of proton pump inhibitors, antidepressants, and antiplatelet agents (Lima et al., 2021), drugs frequently given in elderly Alzheimer's patients. The non-inhibitor status of all reference drugs indicates that CYP2C19 inhibition is not obligate for effective anti-Alzheimer design, and that structural modifications in the synthesized series confer CYP2C19 affinity absent in simpler clinical structures.

CYP2C9, only 8 compounds are predicted CYP2C9 inhibitors, while 28, including all five reference drugs, are non-inhibitors, representing the most favorable inhibition profile in the

dataset. CYP2C9 metabolizes warfarin, NSAIDs, and antidiabetic agents, and its inhibition carries significant hemorrhagic and hypoglycemic DDI risk (Tateishi et al., 2021). The general status in non-inhibitor, both the synthesized series and reference drugs represents a consistent safety advantage, suggesting CYP2C9 non-inhibition is a pharmacokinetically conserved property within this chemical class.

CYP2D6, from Twenty-eight compounds are predicted CYP2D6 inhibitors, while 8 are non-inhibitors: synthesized compounds 3g, 3i, 3l, 7d, and 7j, along with memantine, rivastigmine, and tacrine. CYP2D6 is clinically relevant because donepezil is a CYP2D6 substrate, and its inhibition can elevate donepezil plasma concentrations to toxic levels(Kim et al., 2025). The non-inhibitor classification of five synthesized candidates identifies a subset with potentially reduced DDI liability in combination therapy with donepezil, offering a pharmacokinetic advantage relevant to adjunct therapeutic strategies.

Table 6. The Properties of Compound 3i and 3l

Parameter	Yes / Alert	No / No Alert	Compounds No Alert
P-gp substrate	34	2	Memantine, Rivastigmine
CYP1A2 inhibitor	32	4	Donepezil, Galantamine, Memantine, Rivastigmine
CYP2C19 inhibitor	27	9	3a, 9c, 9e, 9f, Donepezil, Galantamine, Memantine, Rivastigmine, Tacrine
CYP2C9 inhibitor	8	28	3a, 3b, 3c, 3d, 3f, 3g, 3h, 3i, 3k, 3l, 7a, 7b, 7d, 7e, 7f, 7i, 7j, 9a, 9b, 9c, 9d, 9e, 9f, Donepezil, Galantamine, Memantine, Rivastigmine, Tacrine
CYP2D6 inhibitor	28	8	3g, 3i, 3l, 7d, 7j, Memantine, Rivastigmine, Tacrine
CYP3A4 inhibitor	33	3	Galantamine, Memantine, Rivastigmine
PAINS alerts	0	36	-
Brenk alerts	1	35	Galantamine

CYP3A4: Thirty-three compounds are predicted CYP3A4 inhibitors; only galantamine, memantine, and rivastigmine are non-inhibitors. As the most abundantly expressed hepatic CYP isoform, responsible for the metabolism of 50% of marketed drugs (Zhang et al., 2024). Its broad inhibition across the series, shared with donepezil and tacrine, suggests a generalized DDI liability intrinsic to the compound class. The non-inhibitor status of galantamine, memantine, and rivastigmine is consistent with their lower LogP and MW, reinforcing the established principle that CYP3A4 inhibition is disproportionately associated with higher lipophilicity and molecular size.

Conclusion

This study evaluated the drug-likeness, ADMET profiles, and BBB penetration potential of 31 indoloquinoxaline derivatives alongside five reference anti-Alzheimer drugs (donepezil, galantamine, memantine, rivastigmine, and tacrine) using SwissADME as a unified computational platform. All 36 compounds demonstrated full compliance with Lipinski's Rule of Five and the Veber filter (100%), while Ghose, Egan, and Muegge filters identified 3, 2, and 8 violations respectively, primarily attributable to excessive lipophilicity conferred by $-CF_3$ and tert-butyl substituents in compounds 3i and 3l. The Consensus LogP values across the synthesized series ranged from 2.88 to 4.95, predominantly within the optimal CNS window, and TPSA values (30.71–54.50 $Å^2$) consistently fell below the 90 $Å^2$ CNS permeability threshold. A total of 29 out of 31 synthesized compounds (93.5%) were predicted as BBB-permeant by the SwissADME. CYP450 inhibition profiling revealed widespread CYP1A2 and CYP3A4 inhibitory activity across the series, warranting consideration for drug–drug interaction risk in polypharmacy settings common to Alzheimer's patients, while CYP2C9 non-inhibition was broadly conserved. These

findings establish a comprehensive SwissADME-based pharmacokinetic baseline for the indoloquinoxaline scaffold and provide a structured framework for CNS-focused lead optimization of this compound class.

Acknowledgments

The authors sincerely acknowledge all research team members for their valuable contributions, collaboration, and support throughout this research.

Conflicts of interest

The authors declare that there are no conflicts of interest regarding the publication of this research.

References

Basagni, F., Ortega, J. A., Bertozzi, S. M., Armirotti, A., Summa, M., Bertorelli, R., Bartolini, M., Mellor, I. R., Bedeschi, M., Bottegoni, G., Lembo, V., Minarini, A., Cavalli, A., & Rosini, M. (2023). Galantamine-memantine hybrids for Alzheimer's disease: The influence of linker rigidity in biological activity and pharmacokinetic properties. *European Journal of Medicinal Chemistry*, *261*. https://doi.org/10.1016/j.ejmech.2023.115803

Bitew, M., Desalegn, T., Demissie, T. B., Belayneh, A., Endale, M., & Eswaramoorthy, R. (2021). Pharmacokinetics and drug-likeness of antidiabetic flavonoids: Molecular docking and DFT study. *PLoS ONE*, *16*(12 December). https://doi.org/10.1371/journal.pone.0260853

Cornelissen, F. M. G., Markert, G., Deutsch, G., Antonara, M., Faaij, N., Bartelink, I., Noske, D., Vandertop, W. P., Bender, A., & Westerman, B. A. (2023). Explaining Blood-Brain Barrier Permeability of Small Molecules by Integrated Analysis of Different Transport Mechanisms. *Journal of Medicinal Chemistry*, *66*(11), 7253–7267. https://doi.org/10.1021/acs.jmedchem.2c01824

Dehnbostel, F. O., Dixit, V. A., Preissner, R., & Banerjee, P. (2024). Non-animal models for blood–brain barrier permeability evaluation of drug-like compounds. *Scientific Reports*, *14*(1). https://doi.org/10.1038/s41598-024-59734-9

Evangelista, T. C. S., López, Ó., Ferreira, S. B., Fernández-Bolaños, J. G., Sydnes, M. O., & Lindbäck, E. (2021). Development of tacrine clusters as positively cooperative systems for the inhibition of acetylcholinesterase. *Journal of Enzyme Inhibition and Medicinal Chemistry*, *36*(1), 1659–1664. https://doi.org/10.1080/14756366.2021.1954917

Gupta, M., Feng, J., & Bhisetti, G. (2024). Experimental and Computational Methods to Assess Central Nervous System Penetration of Small Molecules. In *Molecules* (Vol. 29, Number 6). Multidisciplinary Digital Publishing Institute (MDPI). https://doi.org/10.3390/molecules29061264

Hamulakova, S., Kudlickova, Z., Janovec, L., Mezencev, R., Deckner, Z. J., Chernoff, Y. O., Janockova, J., Ihnatova, V., Bzonek, P., Novakova, N., Hepnarova, V., Hrabinova, M., Jun, D., Korabecny, J., Soukup, O., & Kuca, K. (2021). Design and synthesis of novel tacrine-indole hybrids as potential multitarget-directed ligands for the treatment of Alzheimer's disease. *Future Medicinal Chemistry*, *13*(9), 785–804. https://doi.org/10.4155/fmc-2020-0184

Hathcock, S. F., Knight, H. E., Tong, E. G., Meyer, A. E., Mauser, H. D., Vollmuth, N., & Kim, B. J. (2024). Induction of P-glycoprotein overexpression in brain endothelial cells as a model to study blood-brain barrier efflux transport. *Frontiers in Drug Delivery*, *4*. https://doi.org/10.3389/fddev.2024.1433453

Hossam Abdelmonem, B., Abdelaal, N. M., Anwer, E. K. E., Rashwan, A. A., Hussein, M. A., Ahmed, Y. F., Khashana, R., Hanna, M. M., & Abdelnaser, A. (2024). Decoding the Role of CYP450 Enzymes in Metabolism and Disease: A Comprehensive Review. In *Biomedicines* (Vol. 12,

Number 7). Multidisciplinary Digital Publishing Institute (MDPI). https://doi.org/10.3390/biomedicines12071467

Janicka, M., Sztanke, M., & Sztanke, K. (2024). Modeling the Blood-Brain Barrier Permeability of Potential Heterocyclic Drugs via Biomimetic IAM Chromatography Technique Combined with QSAR Methodology. *Molecules*, *29*(2). https://doi.org/10.3390/molecules29020287

Kenny, P. W. (2022). Hydrogen-Bond Donors in Drug Design. In *Journal of Medicinal Chemistry* (Vol. 65, Number 21, pp. 14261–14275). American Chemical Society. https://doi.org/10.1021/acs.jmedchem.2c01147

Khwaza, V., Oyedeji, O. O., Morifi, E., Nwamadi, M., Fonkui, T. Y., Ndinteh, D. T., & Aderibigbe, B. A. (2025). Design and Synthesis of Hybrid Compounds for Potential Treatment of Bacterial Co-Infections: In Vitro Antibacterial and In Silico Studies. *Antibiotics*, *14*(6). https://doi.org/10.3390/antibiotics14060582

Kim, T. E., Bae, J. W., Hong, S., Jeon, H. J., & Moon, Y. (2025). The impact of CYP2D6 on donepezil concentration and its lack of effect on the treatment response and adverse effect in Korean patients with Alzheimer's disease. *Korean Journal of Physiology and Pharmacology*, *29*(2), 227–233. https://doi.org/10.4196/kjpp.24.239

Kralj, S., Jukič, M., & Bren, U. (2023). Molecular Filters in Medicinal Chemistry. *Encyclopedia*, *3*(2), 501–511. https://doi.org/10.3390/encyclopedia3020035

Lambev, M., Dimitrova, D., & Mihaylova, S. (2025). Machine Learning-Based Prediction of Rule Violations for Drug-Likeness Assessment in Peptide Molecules Using Random Forest Models. *International Journal of Molecular Sciences*, *26*(17). https://doi.org/10.3390/ijms26178407

Lima, J. J., Thomas, C. D., Barbarino, J., Desta, Z., Van Driest, S. L., El Rouby, N., Johnson, J. A., Cavallari, L. H., Shakhnovich, V., Thacker, D. L., Scott, S. A., Schwab, M., Uppugunduri, C. R. S., Formea, C. M., Franciosi, J. P., Sangkuhl, K., Gaedigk, A., Klein, T. E., Gammal, R. S., & Furuta, T. (2021). Clinical Pharmacogenetics Implementation Consortium (CPIC) Guideline for CYP2C19 and Proton Pump Inhibitor Dosing. *Clinical Pharmacology and Therapeutics*, *109*(6), 1417–1423. https://doi.org/10.1002/cpt.2015

Mahmud, S., Paul, G. K., Biswas, S., Kazi, T., Mahbub, S., Mita, M. A., Afrose, S., Islam, A., Ahaduzzaman, S., Hasan, R., Shimu, S. S., Promi, M. M., Shehab, M. N., Rahman, E., Sujon, K. M., Alom, W., Modak, A., Zaman, S., Uddin, S., … Saleh, A. (2022). phytochemdb: a platform for virtual screening and computer-aided drug designing. *Database*, *2022*(2022). https://doi.org/10.1093/database/baac002

Merino, D., Fernandez, A., Gérard, A. O., Othman, N. Ben, Rocher, F., Askenazy, F., Verstuyft, C., Drici, M. D., & Thümmler, S. (2022). Adverse Drug Reactions of Olanzapine, Clozapine and Loxapine in Children and Youth: A Systematic Pharmacogenetic Review. In *Pharmaceuticals* (Vol. 15, Number 6). MDPI. https://doi.org/10.3390/ph15060749

Miebs, G., Mielniczuk, A., Kadziński, M., & Bachorz, R. A. (2024). Beyond the Arbitrariness of Drug-Likeness Rules: Rough Set Theory and Decision Rules in the Service of Drug Design. *Applied Sciences (Switzerland)*, *14*(21). https://doi.org/10.3390/app14219966

Pajouhesh, H., & Lenz, G. R. (n.d.). *Medicinal Chemical Properties of Successful Central Nervous System Drugs*.

Rashid, M., Athar, M. T., Abdelmageed, M., Al-Harbi, M. H. M., Husain, A., Bisht, D., & Arya, R. K. K. (2023). Silver Nanoparticles from Saudi and Syrian Black Cumin Seed Extracts: Green Synthesis, ADME, Toxicity, Comparative Research, and Biological Appraisal. *Journal of Pharmacy and Bioallied Sciences*, *15*(4), 190–196. https://doi.org/10.4103/jpbs.jpbs_381_23

Reddi Sree, R., Kalyan, M., Anand, N., Mani, S., Gorantla, V. R., Sakharkar, M. K., Song, B. J., & Chidambaram, S. B. (2025). Newer Therapeutic Approaches in Treating Alzheimer's Disease: A Comprehensive Review. In *ACS Omega* (Vol. 10, Number 6, pp. 5148–5171). American Chemical Society. https://doi.org/10.1021/acsomega.4c05527

Ronaldson, P. T., & Davis, T. P. (2024). Blood–brain barrier transporters: a translational consideration for CNS delivery of neurotherapeutics. In *Expert Opinion on Drug Delivery* (Vol.

21, Number 1, pp. 71–89). Taylor and Francis Ltd. https://doi.org/10.1080/17425247.2024.2306138

Sampat, G., Suryawanshi, S. S., Palled, M. S., Patil, A. S., Khanal, P., & Salokhe, A. S. (2022). Drug Likeness Screening and Evaluation of Physicochemical Properties of Selected Medicinal Agents by Computer Aided Drug Design Tools. *Advances in Pharmacology and Pharmacy*, *10*(4), 234–246. https://doi.org/10.13189/app.2022.100402

Shityakov, S., Neuhaus, W., Dandekar, T., & Förster, C. (2013). Analysing molecular polar surface descriptors to predict blood-brain barrier permeation. *International Journal of Computational Biology and Drug Design*, *6*(1–2), 146–156. https://doi.org/10.1504/IJCBDD.2013.052195

Staneva, Y., Iliev, I., Georgieva, S., & Merdjanova, A. (2024). In silico prediction of physicochemical properties and drug-likeness of omega-3 fatty acids . *Ovidius University Annals of Chemistry*, *35*(2), 118–125. https://doi.org/10.2478/auoc-2024-0016

Tateishi, H., Miyazu, D., Kurinami, M., Ieiri, I., Hirakawa, M., & Watanabe, H. (2021). Hypoglycemia possibly caused by CYP2C9-mediated drug interaction in combination with bucolome: a case report. *Journal of Pharmaceutical Health Care and Sciences*, *7*(1). https://doi.org/10.1186/s40780-021-00221-y

Vawhal, P. K., & Jadhav, S. B. (2022). Design, synthesis, and biological evaluation of 3-chloro-2-oxo-N-(arylcarbamoyl)-2H-1-benzopyran-6-sulfonamide derivatives as potential DPP-IV inhibitors. *International Journal of Health Sciences*, 373–392. https://doi.org/10.53730/ijhs.v6ns3.5190

Veber, D. F., Johnson, S. R., Cheng, H. Y., Smith, B. R., Ward, K. W., & Kopple, K. D. (2002). Molecular properties that influence the oral bioavailability of drug candidates. *Journal of Medicinal Chemistry*, *45*(12), 2615–2623. https://doi.org/10.1021/jm020017n

Xiong, B., Wang, Y., Chen, Y., Xing, S., Liao, Q., Chen, Y., Li, Q., Li, W., & Sun, H. (2021). Strategies for Structural Modification of Small Molecules to Improve Blood-Brain Barrier Penetration: A Recent Perspective. In *Journal of Medicinal Chemistry* (Vol. 64, Number 18, pp. 13152–13173). American Chemical Society. https://doi.org/10.1021/acs.jmedchem.1c00910

Zhang, Y., Wang, Z., Wang, Y., Jin, W., Zhang, Z., Jin, L., Qian, J., & Zheng, L. (2024). CYP3A4 and CYP3A5: the crucial roles in clinical drug metabolism and the significant implications of genetic polymorphisms. In *PeerJ* (Vol. 12, Number 12). PeerJ Inc. https://doi.org/10.7717/peerj.18636